Mon. Not. R. Astron. Soc. **357,** 527–534 (2005) doi:10.1111/j.1365-2966.2005.08620.x

The Gaussian cell two-point 'energy-like' equation: application to large-scale galaxy redshift and peculiar motion surveys

Saleem Zaroubi[1]⋆ and Enzo Branchini[2]

[1]*Kapteyn Astronomical Institute, University of Groningen, Landleven 12, 9747 AG Groningen, the Netherlands*
[2]*Dipartimento di Fisica dell' Università degli Studi 'Roma TRE', Via della Vasca Navale 84, I-00146, Roma, Italy*

Accepted 2004 November 8. Received 2004 October 27; in original form 2004 July 21

ABSTRACT

We introduce a simple linear equation relating the line-of-sight peculiar-velocity and density contrast correlation functions. The relation, which we call the *Gaussian cell two-point 'energy-like' equation*, is valid at the distant-observer limit and requires Gaussian smoothed fields. In the variance case, i.e. at zero lag, the equation is similar in its mathematical form to the Irvine–Layzer cosmic energy equation. β estimation with this equation from the Point Source Catalogue Redshift (PSC) survey and the SEcat catalogue of peculiar velocities is carried out, returning a value of $\beta = 0.44 \pm 0.08$. The applicability of the method for the 6dF galaxy redshift and peculiar motions survey is demonstrated with mock data where it is shown that β could be determined with $\approx$10 per cent accuracy. The prospects for constraining the dark energy equation of state with this method from the kinematic and thermal Sunyaev–Zel'dovich cluster surveys are discussed. The equation is also used to construct a non-parametric mass-density power-spectrum estimator from peculiar-velocity data.

Key words: galaxies: clusters: general – galaxies: distances and redshifts – cosmological parameters – cosmology: theory – large-scale structure of Universe.

1 INTRODUCTION

In the linear regime of the gravitational instability scenario, the underlying mass distribution is directly traced by the galaxy peculiar velocities. Measurement of the radial component of the galaxy peculiar velocities, the only component that one can easily observe, is carried out with one of many available techniques, the most common among which are the Tully–Fisher-like methods (e.g. Tully & Fisher 1977; Faber & Jackson 1976). Normally, these methods exploit a well-defined intrinsic relation between two or more of the galaxy[1] observed properties that facilitates establishing its actual distance from the observer. The estimated distance is then used together with the measured galaxy redshift, to determine the galaxy radial peculiar velocity. Assuming an irrotational flow on large scales and knowledge of $\Omega_{\rm m}$ (the cosmological mass-density parameter), it is straightforward to use the measured radial peculiar velocities to recover the full underlying mass overdensity (Bertschinger & Dekel 1989; Dekel, Bertschinger & Faber 1990; Zaroubi 2002; Zaroubi et al. 2002). In addition, the same mass density could be probed by galaxy redshift catalogues assuming a simple linear biasing scheme that connects it to the spatial galaxy distribution (Kaiser 1984; Bardeen et al. 1986). To date, galaxy redshift and peculiar motion surveys are the main tools with which astronomers explore the distribution of matter in the nearby Universe.

Since the two types of data, galaxy peculiar-velocity catalogues and galaxy redshift surveys, probe the underlying mass distribution, comparing the two provides a simple and powerful test of the paradigm of gravitational instability and gives a model-independent measurement of β, the ratio between the linear growth factor, $f(\Omega_{\rm m})$ ($\approx \Omega_{\rm m}^{0.6}$), and the linear biasing factor of the galaxy population. In most cases the comparison is either performed by deriving galaxy peculiar velocities from the galaxy density field and confronting them with the measured velocities point-by-point, an approach usually called 'velocity–velocity' comparison (e.g. Davis, Nusser & Willick 1996; Willick & Strauss 1998; Zaroubi 2002; Zaroubi et al. 2002), or by adopting the so-called 'density–density' approach in which the velocity data are used to infer the full mass-density field (Bertschinger & Dekel 1989; Zaroubi 2002) and comparing it with the galaxy distribution (e.g. Sigad et al. 1998; Zaroubi et al. 2002). With the exception of the POTENT algorithm (see, e.g. Sigad et al. 1998), all the comparison methods yield a low value of β consistent with $\Omega_{\rm m} \approx 0.3$ and bias factor of $\approx$1.

Another approach to the comparison that does not fit into the two general classes outlined earlier is the one proposed by Juszkiewicz et al. (2000) who start from the pair conservation equation (Peebles 1980) and evolve it further to the quasi-linear regime of gravitational instability. In the pair conservation approach, which yields

⋆E-mail: saleem@astro.rug.nl

[1] It should be noted that some methods are not based on galaxy properties and use other 'extragalactic objects', e.g. Type Ia supernovae.

a value of β that is consistent with the one derived from velocity–velocity analyses (Ferreira et al. 1999; Feldman et al. 2003), a relation between the mean pairwise velocity at a certain separation and the density correlation function is derived. The comparison in this approach is significantly simplified by avoiding the spatial point-by-point matching required in previous methods thus reducing the noise involved. The Juszkiewicz et al. (1999) approach is similar to the one developed in this paper except that we are interested in the variance of the peculiar velocity at a given smoothing scale rather than the pairwise peculiar velocity at a given separation.

In this study, we derive a very simple, model-independent and linear relation, valid at the distant-observer limit, between the overdensity and peculiar-velocity two-point correlation functions assuming Gaussian smoothing. The method is first used to construct a non-parametric estimator of the mass-density power spectrum. Then the paper concentrates on the relation between the variance (two-point correlation at zero distance) of the two fields. This relation basically reduces the comparison between the catalogues to two numbers allowing a robust extraction of the parameter β. The proposed equation is especially suited to future peculiar-velocity data sets like the 6dF which will measure the peculiar velocities of 15 000 galaxies with their D_n–σ relation up to 150 h^{-1} Mpc distance.

Currently, the main sources of error in the redshift–peculiar-motion comparison are the large random and systematic uncertainties carried by the peculiar-motion measurements; for example, the Tully–Fisher-like relations have an inherent uncertainty of ≈15–20 per cent of the distance. Data obtained with more accurate distance indicators do exist (Tonry 1991; Riess, Press & Kirshner 1995); unfortunately, however, either they are not at significant distances, e.g. the surface-brightness fluctuations method, or they reach large distances but are too sparse, e.g. the Type Ia supernovae data. In the future, by using the thermal and kinematic Sunyaev–Zel'dovich (SZ) effect (Sunyaev & Zel'dovich 1972), both the accuracy of the peculiar-velocity measurement and the spatial coverage of the data are expected to increase dramatically where the uncertainty is expected to amount to an absolute error of ≈150 km s^{-1} (e.g. Diaferio et al. 2004) and the number of observed objects to reach ≈10^4 clusters. The main difficulty in this case, assuming a reasonable control over the systematics, will be posed by the large mean separation between the galaxy clusters observed with the SZ effect.

The power of the method proposed here is that it reduces the contribution of the measurement noise and sparseness of the sample to a bare minimum. The paper is organized as follows. Section 2 presents the main theoretical formulae. In Section 3 the method is applied to the PSCz redshift galaxy catalogue and the SEcat peculiar-velocity survey. In Section 4 the applicability of the method to future surveys, e.g. the 6dF galaxy survey and the kinematic and thermal SZ cluster survey, is discussed.

2 THEORETICAL DERIVATIONS

In this section, we first derive the main theoretical relation (Section 2.1) and show how it could be used to estimate the matter power spectrum from peculiar-velocity data (Section 2.2). Then in Section 2.3.1 the variance component of the main relation is used in order to estimate the value of β from comparison between galaxy redshift survey data and peculiar-velocity data. The β measurement error for a typical case is derived in Section 2.3.2. The derivation is performed within the framework of linear gravitational instability, under the assumption of statistical homogeneity and isotropy.

2.1 The basic relation

Consider a radial peculiar-velocity field $v_{\rm los}(\boldsymbol{r})$ measured in a very distant patch of the sky smoothed with a Gaussian window function with scale $R_{\rm s}$, $W_{R_{\rm s}}(r) = (2\pi {R_{\rm s}}^2)^{-3/2} \exp(-r^2/2R_{\rm s}^2)$. In the limit of $R_{\rm c} \ll R$, where $R_{\rm c}$ is the correlation radius of peculiar velocities and R is the distance of the patch from the observer, a smoothed radial field within a given observed volume can be written as,

$$v^{\rm S}_{\rm los}(\boldsymbol{x}) = \frac{-\imath\beta H_0}{(2\pi)^3} \int \frac{\hat{\boldsymbol{r}}_{\rm los}\cdot\boldsymbol{k}}{k^2}\delta_k W_{R_{\rm s}}(k) \exp(-\mathrm{i}\boldsymbol{k}\cdot\boldsymbol{x})\,\mathrm{d}^3k, \tag{1}$$

where the superscript 'S' refers to values smoothed with a Gaussian kernel of radius $R_{\rm s}$, $\hat{\boldsymbol{r}}_{\rm los}$ is a unit vector along the line of sight, and $W_{R_{\rm s}}(k)$ is the Fourier transform of the smoothing kernel.

The two-point correlation function of the Gaussian smoothed line-of-sight galaxy peculiar velocity is:

$$\left\langle \xi^{\rm los}_v(\boldsymbol{r}; R_{\rm s})\right\rangle \equiv \left\langle v^{\rm S}_{\rm los}(\boldsymbol{x}) v^{\rm S}_{\rm los}(\boldsymbol{x}+\boldsymbol{r})\right\rangle \tag{2}$$

$$= \frac{\beta^2 H_0^2}{(2\pi)^3} \times \int \frac{(\hat{\boldsymbol{r}}_{\rm los}\cdot\boldsymbol{k})^2}{k^4} P_k W_k^2 \exp(-\mathrm{i}\boldsymbol{k}\cdot\boldsymbol{r})\,\mathrm{d}^3k, \tag{3}$$

where P_k is the mass-density power spectrum and $\boldsymbol{r}$ is the radius vector separating any two points. Since there are two independent directions that appear in equation (3) one cannot invoke symmetry arguments in order to proceed. However, since at the distant-observer limit the line-of-sight direction is approximately constant across the observed volume and independent of the direction of $\boldsymbol{r}$, one can average over all possible directions of $\boldsymbol{r}$ relative to $\boldsymbol{k}$ (arbitrary direction) by integrating equation (3) with $1/2\int_{-1}^{1}\mathrm{d}\mu$, where μ is the cosine the angle between the two vectors $\boldsymbol{r}$ and $\boldsymbol{k}$:

$$\left\langle \xi^{\rm los}_v(\boldsymbol{r}; R_{\rm s})\right\rangle_\mu = \frac{(\beta H_0)^2}{(2\pi)^3} \int (\hat{\boldsymbol{r}}_{\rm los}\cdot\boldsymbol{k})^2 \frac{P_k}{k^4} W_k^2\; j_0(kr)\,\mathrm{d}^3k, \tag{3}$$

where $\langle\,\rangle_\mu$ is an average over the statistical ensemble and over μ, $j_0(kr)$ is the zero-order spherical Bessel function and $r = |\,\boldsymbol{r}\,|$.

Assuming statistical isotropy for the velocity field, i.e. symmetry between the line of sight and the other two orthogonal directions, one obtains the following equation:

$$\left\langle \xi^{\rm los}_v(\boldsymbol{r}; R_{\rm s})\right\rangle_\mu = \frac{\beta^2 H_0^2}{3(2\pi)^3} \int \frac{P_k}{k^2} W_k^2(R_{\rm s}) j_0(kr)\,\mathrm{d}^3k, \tag{5}$$

with the factor 3 coming from a symmetry argument. Now for the last step in the calculation, for a Gaussian smoothing kernel, i.e. $W_{R_{\rm s}}(k) = \exp(-k^2R_{\rm s}^2/2)$, the derivative of the line-of-sight velocity two-point correlation function with respect to $R_{\rm s}$, yields:

$$\frac{\mathrm{d}\left\langle \xi^{\rm los}_v(r; R_{\rm s})\right\rangle_\mu}{\mathrm{d}R_{\rm s}} = -\frac{2}{3}\beta^2 H_0^2 R_{\rm s} \int P_k W_k^2 j_0(kr) \frac{\mathrm{d}^3k}{(2\pi)^3} \tag{6}$$

$$= -\frac{2}{3}\beta^2 H_0^2 R_{\rm s} \xi(r; R_{\rm s}). \tag{7}$$

Here $\xi(r;\,R_{\rm s})$ is the two-point correlation function of the smoothed densities. Notice that equation (7) can only be obtained when $\mathrm{d}W_{R_{\rm s}}(k)/\mathrm{d}R_{\rm s} \propto k^2 W_{R_{\rm s}}(k)$, strictly valid only with a Gaussian smoothing kernel.[2]

[2] There are other functions that satisfy this relation but they do not satisfy the requirements of smoothing kernels.

Obviously, for a given three-dimensional peculiar-velocity field the two-point correlation function of the Gaussian smoothed velocity, $\boldsymbol{v}^{\rm S}$, is related to its density counterpart through the equation,

$$\frac{{\rm d}\langle\xi_v(r;R_{\rm s})\rangle}{{\rm d}R_{\rm s}} \equiv \langle \boldsymbol{v}^{\rm S}(\boldsymbol{x})\cdot\boldsymbol{v}^{\rm S}(\boldsymbol{x}+\boldsymbol{r})\rangle \tag{8}$$

$$= -2\beta^2 H_0^2 R_{\rm s}\xi(r;R_{\rm s}), \tag{9}$$

which is similar to equation (7) without the factor of 3 and with no need for averaging over μ.

It might be easier to interpret equation (7) in its integral form, where the integral is performed over the smoothing radius. Let R_1 and R_2 be the two smoothing radii that bound our integral. Then,

$$\frac{1}{2}\left\langle\xi_v^{\rm los}(r;R_{\rm s})\right\rangle_\mu\Big|_{R_1}^{R_2} = -\frac{\beta^2}{3}H_0^2\int_{R_1}^{R_2}\frac{\xi(r;R_{\rm s})}{R_{\rm s}}\frac{{\rm d}^3R_{\rm s}}{4\pi}. \tag{10}$$

In the limit $r=0$, the left-hand side of equation (10) describes the mean change in the kinetic energy associated with the smoothed velocity due to the variation of the smoothing radius, whereas the right-hand side depicts the three-dimensional integral of the density variance of the smoothed field over the smoothing scale. The right-hand side term is very similar to the normal potential energy except that $R_{\rm s}$ does not represent a proper distance between points. In other words, the variation in the kinetic-like energy comes from the 'potential energy like' behaviour of the modes corresponding to the scales between R_1 and R_2, with exponentially decreasing contributions from larger and smaller scale modes. If $r\neq 0$ then the interpretation is not as simple but still the left- and right-hand sides correspond to a sort of *two-point kinetic energy* and *potential energy*, respectively, with the same scales contributing to the modification as before. Therefore, equation (10) is an 'energy equation' of sorts as it describes the *two-point* 'potential-like' and 'kinetic-like' energy partition within a Gaussian window function. Dimensional arguments significantly restrict the mathematical form of the relation between the velocity and the density two-point correlation functions. Therefore, it is not surprising that the theoretical relation shown by equation (7) is very similar to the Irvine–Layzer cosmic energy equation which describes how the energy of the Universe is partitioned between kinetic and potential energy (Irvine 1961, 1965; Layzer 1963, 1966; see also Mo, Jing & Börner 1997).

2.2 The mass-density power spectrum

The main approach currently used to measure the mass-density power spectrum from peculiar-velocity data is the likelihood method introduced by Zaroubi et al. (1997; see also, Freudling et al. 1999 and Zaroubi et al. 2001) in which a theoretical power spectrum with few free parameters and a noise model are assumed. Since in this method the data are forced to fit a specific power-spectrum shape, an inaccurate description of the noise model could propagate to large scales and contaminate the measured power spectrum. Indeed the results obtained with this method have been yielding unrealistically high amplitudes of the mass-density fluctuation power spectrum (consistent with $\Omega_{\rm m}>0.6$). Therefore, direct non-parametric methods for power-spectrum estimation from peculiar-velocity data are needed.

The question we pose here is: can equation (7) be used to estimate directly the mass power spectrum from peculiar-velocity data? In the ideal case in which the uncertainties in the measurement are neglected and the data extends to infinity and samples the Universe very accurately, the answer is clearly yes.

A good point from which to start the derivation of the power-spectrum estimator is the relation between the power spectrum and the smoothed density two-point correlation function,

$$\xi(r;R_{\rm s}) = \frac{1}{2\pi^2}\int P_{k'}\exp\left(-k^2R_{\rm s}^2\right)j_0(k'r)k'^2\,{\rm d}k'. \tag{11}$$

Substituting this into equation (7) and integrating over the variable r from zero to ∞ after multiplying by $j_0(kr)\,r^2$, one obtains the following relation,

$$\frac{6\pi}{H_0^2R_{\rm s}}\int_0^\infty\frac{{\rm d}\left\langle\xi_v^{\rm los}(r;R_{\rm s})\right\rangle_\mu}{dR_{\rm s}}j_0(kr)r^2\,{\rm d}r = f^2P_k\exp(-k^2R_{\rm s}^2), \tag{12}$$

where the orthonormality of the spherical Bessel function is used (e.g. Arfken & Weber 2001). The left-hand side of equation (12) is a quantity that can be directly measured from the velocity data, whereas the right-hand side shows the estimated quantity. Since we use smoothed velocity data, the power spectrum is determined up to a factor of $f^2(\Omega_{\rm m})$ and with a resolution that cannot exceed the scale imposed by the Gaussian smoothing.

For a real application, the discrete and noisy nature of the data should be taken into account, i.e. some of the steps leading to equation (12) have to be modified. For example, to maintain the orthogonality of the spherical Bessel functions on a finite spherical volume one has to impose appropriate boundary conditions (see Fisher et al. 1995; Zaroubi et al. 1995, for examples). However, the main hurdle for this direct approach to power-spectrum estimation is the noise contribution; this issue is deferred to future work.

2.3 Estimation of β

2.3.1 Estimator

Equation (7) is the most general relation derived in this paper. However, in order to use it to estimate the value of β, it is simpler to restrict ourselves to the relation between the density and velocity variances, namely, apply the equation in the limiting case of $\boldsymbol{r}=\boldsymbol{0}$ to yield:

$$\frac{{\rm d}\sigma_{\rm v}^2(R_{\rm s})}{{\rm d}R_{\rm s}} = -\frac{2}{3}\beta^2H_0^2R_{\rm s}\sigma_\delta^2(R_{\rm s}), \tag{13}$$

where $\sigma_{\rm v}^2$ and σ_δ^2 are the peculiar-velocity and density-contrast variances, respectively.

The numerical calculation of ${\rm d}\sigma_{\rm v}^2(R_{\rm s})/{\rm d}R_{\rm s}$ is straightforward. One has to smooth the measured velocity field with a Gaussian window, calculate its variance and obtain its derivative by finite differencing (see Section 2.3.2 for a similar explicit calculation). The right-hand side of equation (13) is obtained from the galaxy redshift catalogue by taking the variance of the smoothed real-space density field.

The proposed estimator requires no heavy data manipulation and is easy to calculate. As a result of the smoothing involved, the estimator is robust with regard to instabilities caused by the large random noise. In addition, to avoid the cosmic variance contribution to the error analysis, the comparison between the two types of data sets is performed within the same region of space. Both features, simplicity and stability, render the estimator very appealing to use.

2.3.2 Noise

The contribution of the measurement error to the estimator in equation (13) is readily calculated with the following discrete approach.

Let $\epsilon(\boldsymbol{r}_i)$ be the noise associated with particle i. Then the smoothed noise is,

$$\epsilon^{\rm S}(\boldsymbol{r}_i) = \sum_l \epsilon(\boldsymbol{r}_l) W_{R_{\rm s}}(\boldsymbol{r}_i - \boldsymbol{r}_l). \tag{14}$$

Subsequently, the expectation value of the noise two-point correlation is,

$$\left\langle \epsilon^{\rm S}(\boldsymbol{r}_i)\epsilon^{\rm S}(\boldsymbol{r}_j)\right\rangle = \sum_l \langle \epsilon^2(\boldsymbol{r}_l)\rangle W_{R_{\rm s}}(\boldsymbol{r}_i - \boldsymbol{r}_l) W_{R_{\rm s}}(\boldsymbol{r}_j - \boldsymbol{r}_l). \tag{15}$$

The last equation assumes that the measured errors are statistically uncorrelated.

We now require that $\boldsymbol{r}_i = \boldsymbol{r}_j$ and sum over all the data points. The expectation value of the noise contribution to the variance of the velocity is

$$\sigma_N^2(R_{\rm s}) = \frac{1}{N}\sum_{i,l} \left\langle \epsilon^2(\boldsymbol{r}_l)\right\rangle W_{R_{\rm s}}^2(\boldsymbol{r}_i - \boldsymbol{r}_l). \tag{16}$$

Therefore, the noise variance that adds to the left-hand side of equation (13) is readily obtained by finite differencing:

$$\frac{{\rm d}\sigma_N^2(R_{\rm s})}{{\rm d}R_{\rm s}} \approx \frac{\sigma_N^2(R_{\rm s}+\Delta R_{\rm s}) - \sigma_N^2(R_{\rm s})}{\Delta R_{\rm s}}. \tag{17}$$

The contribution of the noise variance to the right-hand side of equation (13) is typically small and is neglected here. However, it is straightforward to account for in the case of unusually noisy data.

3 COMPARISON BETWEEN THE SEcat AND THE PSCz CATALOGUES

In this section equation (13) is employed for comparison between the PSCz galaxy redshift catalogue (Branchini et al. 2000; Saunders et al. 2000) and the SEcat galaxy peculiar-velocity catalogue (Zaroubi et al. 2002) which is a combination of the two homogeneous peculiar-velocity catalogues, the SFI catalogue of spiral galaxies (Giovanelli et al. 1998; Haynes et al. 1999) and the ENEAR catalogue of early-type galaxies (da Costa et al. 2000). The SEcat catalogue extends to a distance of about 70 h^{-1} Mpc and the PSCz goes to about twice that. Therefore, in order to avoid cosmic variance contamination of the measurement, the comparison between the two is restricted to the closer distance.

Prior to applying the method to the actual data, however, one needs to address the question of whether it is realistic to expect a reliable estimation of the value of β when using a noisy and local catalogue such as the SEcat. Hence, the next subsection is dedicated to testing with mock catalogues how robust our estimator is.

3.1 Testing with mock data

The density and peculiar-velocity mock catalogues used in this section are derived from the 3.2 h^{-1} Mpc resolution reconstruction of the density field from the PSCz galaxy redshift catalogue (Branchini et al. 2000), where the peculiar-velocity field is obtained using linear theory from the galaxy redshift space positions assuming a value of $\beta = 0.5$. The mock SEcat peculiar-velocity catalogue has the same distances and number of points that the real SEcat has, but with the velocities of the PSCz reconstructed velocity field. Obviously, it would have been better to use a full non-linear N-body simulation with which to test the method. However, since the positions of the actual measured velocities are controlled by the specific distribution of the galaxies in the nearby Universe we choose to test the method with data that have the same spatial distribution as the real Universe, albeit the lack of full non-linearity. Given the heavy smoothing involved in the analysis this way of assigning velocities to mock data is satisfactory – for testing the method with full non-linear simulation see Section 4. After assigning the velocities to the noise-free mock data, we generate 30 mock catalogues with the random errors added to their distance and velocity values in concordance with the observational uncertainties.

However, as a first step we wish to test whether the method works at the distant-observer limit with homogeneous sampling and noise-free data. In this case we have constructed the mock velocity data by sampling the PSCz catalogue on every eighth grid point where the velocity is taken to be equal to the z-component to mimic the distant-observer limit. Fig. 1 shows β as a function of the smoothing scale (dotted-dashed line) which agrees quite well, especially at larger smoothing scales, with the expected value shown with the dotted horizontal line.

Next, the same mock data are used but the peculiar velocity is chosen to be the radial velocity, i.e. the distant-observer limit is relaxed. The points that were chosen for the comparison are restricted to the range $30 < r < 60\ h^{-1}$ Mpc from the centre of the box (relaxing this restriction alters the results but marginally). The result of this test is shown as a dashed line in Fig. 1 indicating that the recovered β is in agreement with its original value.

The third issue to test is whether the spatial coverage of the data set is sufficient, namely, whether the number of SEcat galaxies and their actual sky distribution are good enough for a recovery of the β value. The answer is given by the solid line in Fig. 1, clearly showing that at small smoothing scales, β is underestimated, then it increases with the smoothing radius until the correct value is recovered on scales larger than 18 h^{-1} Mpc. Here the positions of the mock velocity

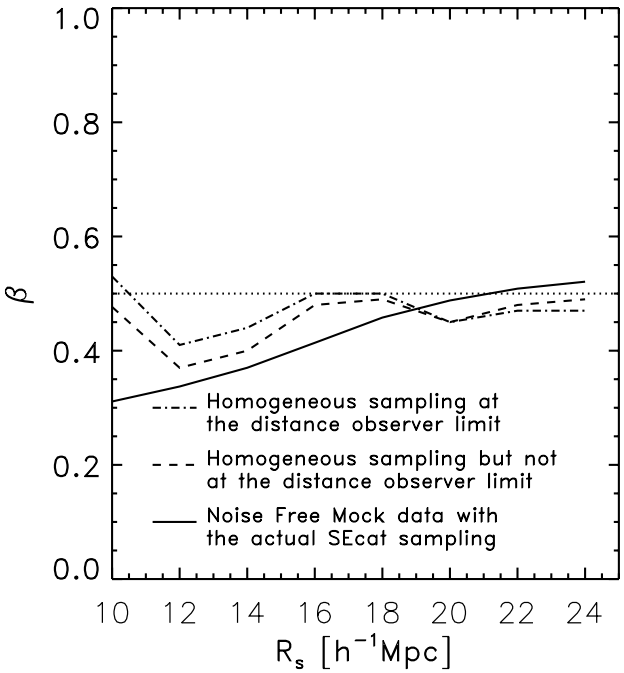

Figure 1. β as deduced from mock velocity data (as taken from PSCz high-resolution data) designed to test various selection effects. The dotted-dashed curve shows β as calculated from a homogeneously sampled velocity catalogue at the distant-observer limit. The dashed line shows β from a homogeneously sampled velocity catalogue but with the actual volume coverage of SEcat, i.e. the distant-observer limit requirement is relaxed. The solid line is β as deduced from noise-free mock peculiar-velocity data with the same selection effects as SEcat. The dotted line shows the correct value of β.

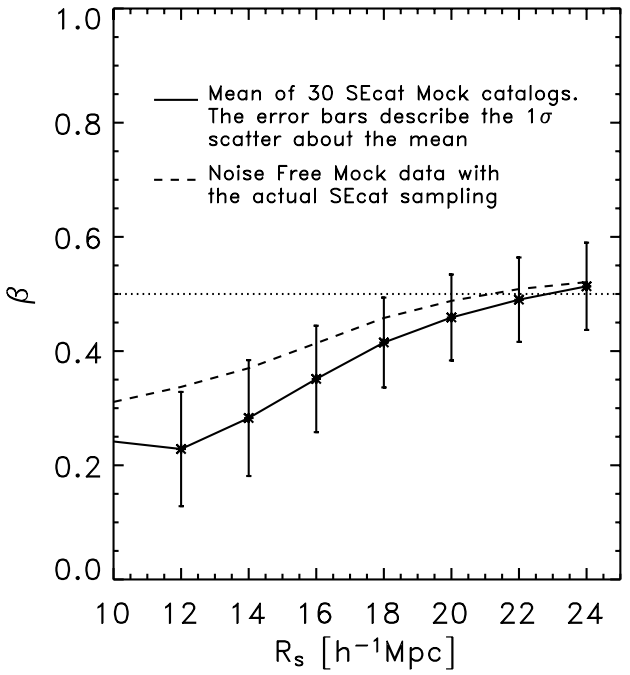

Figure 2. β as deduced from mock SEcat data where the underlying β in this catalogues is 0.5 (dotted line). The solid line shows the mean β as obtained from 30 SEcat mock catalogues with the error bars reflecting the 1σ uncertainty around the mean. The dashed line shows the recovered value of β for the noise-free case; clearly, there is an underestimation of β from the noisy data at small smoothing radii.

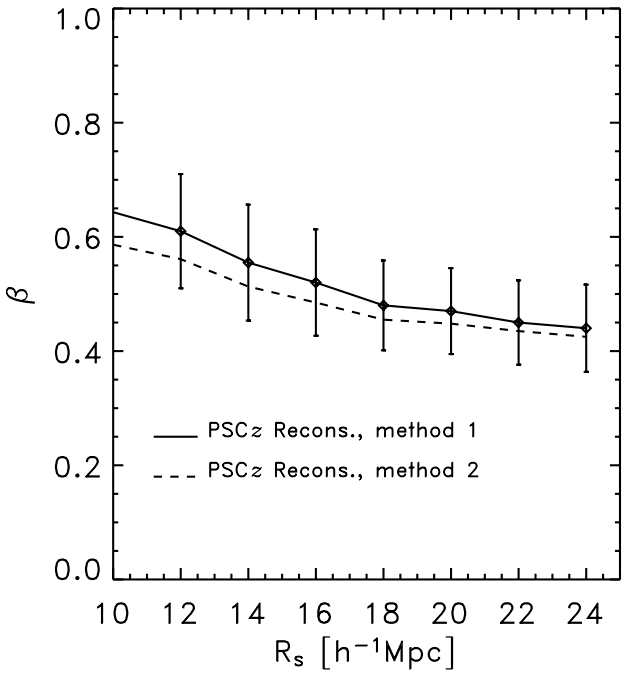

Figure 3. β as deduced from comparison of the real SEcat data with PSCz. The solid line and dashed line reflect results from different assumptions from the density reconstruction. The error bars reflect the 1σ uncertainty.

data are the same as the galaxy positions in the SEcat catalogue but their velocities are taken from the PSCz velocity field with no noise addition.

One might argue that there is no clear convergence of the value of β at $R_s = 24\ h^{-1}$ Mpc in Fig. 1, therefore, one might need to go to larger scales. However, given the size of the current velocity data catalogues, larger scale smoothing becomes comparable to the volume of the data set itself and one has to start to worry about sampling issues within the Gaussian kernel itself. As will be shown later the convergence is also an issue, albeit less severe, for the real data.

The final step in our testing is to apply the method to a 'full' mock SEcat catalogue (with noise and actual sampling). The solid line in Fig. 2 shows the mean value of β as a function of the smoothing radius as recovered from 30 mock SEcat catalogues with the error bars indicating the 1 σ scatter about the mean. β is clearly well reconstructed with large smoothing radii. There is also some bias in the mean value of β at the smaller smoothing radii with respect to the β obtained from the noise-free data (dashed line), which is probably due to overestimation of the noise variance at smaller scales. This is not a big worry as on small scales the PSCz catalogue used to produce the velocity data has limited non-linear evolution due to its poor resolution ($3.2\ h^{-1}$ Mpc) and its velocities are purely linear.

Please note that the error bars shown here are correlated. The uncertainty estimates made for this figure, and for the rest of the figures in the paper, are based on one of the error bars and not their combination.

3.2 β from the real data

Having tested the method on mock catalogues and demonstrated that, on large scales, it gives unbiased results for a SEcat–PSCz comparison, we now apply it to the real data. Fig. 3 shows the measured β as a function of the smoothing radius where it has a value of 0.6 at smoothing radius of $10\ h^{-1}$ Mpc but drops down as the smoothing radius increases to $\approx$0.45; the curve becomes almost flat at $R_s \gtrsim 18\ h^{-1}$ Mpc. The error bars here are taken from the 1σ uncertainties determined from the 30 mock catalogues.

Branchini et al. (2000) have used two methods to solve for the redshift distortion equation (Kaiser 1987) and reconstructed the real-space density from the PSCz galaxy redshift distribution. One is based on the Yahil et al. (1991) iterative method and the other on the Nusser & Davis (1994) spherical harmonic expansion approach. In the previous analysis we have used data obtained with the former method. However, to examine the robustness of the measured value of β we perform the same comparison but with the latter method. The dashed line in Fig. 3 shows β as a function of smoothing radius deduced from the second method which is well within the 1σ uncertainty level, albeit being slightly smaller.

On small smoothing scales the behaviour of the curves shown in Fig. 3 is systematically different from those obtained from the analysis of the mock catalogues; the former drops with scale while the later increases. We attribute this difference to the fact that the PSCz catalogue has a limited resolution and its velocity field is purely linear.

4 FUTURE SURVEYS

4.1 Application to the mock 6dF catalogue

In the near future, the 6dF Galaxy Survey (Jones et al. 2004) will measure the redshifts of around 150 000 galaxies, and the peculiar velocities of a 15 000-member subsample, over almost the entire southern sky. When complete, it will be the largest redshift survey of the nearby Universe, reaching out to about $z \approx 0.15$, and more than an order of magnitude larger than any peculiar-velocity survey to

date. Since the two data sets will be obtained from the same survey, the galaxy redshift and peculiar-velocity catalogues will have the valuable attribute of being subjected to the same selection effects.

Despite the relatively large volume covered by the 6dF galaxy peculiar-velocity survey the relative nature of the errors in the D_n–σ distance estimation might still diminish the information content of the data. To evaluate this effect we apply equation (13) to mock 6dF galaxy redshift and peculiar-velocity catalogues. In this experiment the catalogues are constructed from the full non-linear N-body numerical simulation described by Cole et al. (1999), specifically, the simulation labelled L3S in their paper. The simulation assumes a CDM power spectrum of fluctuations with $\Omega_{\rm m} = 0.3$, $\Lambda = 0.7$, rms fluctuation of the mass contained in spheres of radius 8 h^{-1} Mpc, $\sigma_8 = 1.13$ and a CDM power-spectrum shape parameter, Γ, of 0.25. The simulation box side is 345.6 h^{-1} Mpc and has 192^3 particles. The mock catalogues were produced by carving out six hemispheres of radius 150 h^{-1} Mpc of the simulation box. We obtain the redshift and peculiar-velocity catalogues with uniform sampling of the galaxies in the simulated hemisphere in accordance with the expected sampling of the 6dF survey. The real-space distribution is presumed to have negligible errors, but the distances in the peculiar-velocity catalogues carry errors of 20 per cent of their actual values. The input linear bias factor, b, is 1.

The star symbols in Fig. 4 show the average β value recovered from the 12 mock catalogues, as a function of smoothing scale. The error bars show the associated variance. The continuous line shows the average β value recovered from the same 12 mock catalogues in which no errors have been added to velocities. Clearly, the recovered β is close to its input value at all smoothing scales. If the error level we get is realistic the accuracy with which the 6dF galaxy survey will recover the β parameter (≈ 0.05) is indeed encouraging.

The recovery of β down to 5 h^{-1} Mpc scale is very encouraging too as it indicates that the Gaussian cell 'energy-like' equation holds

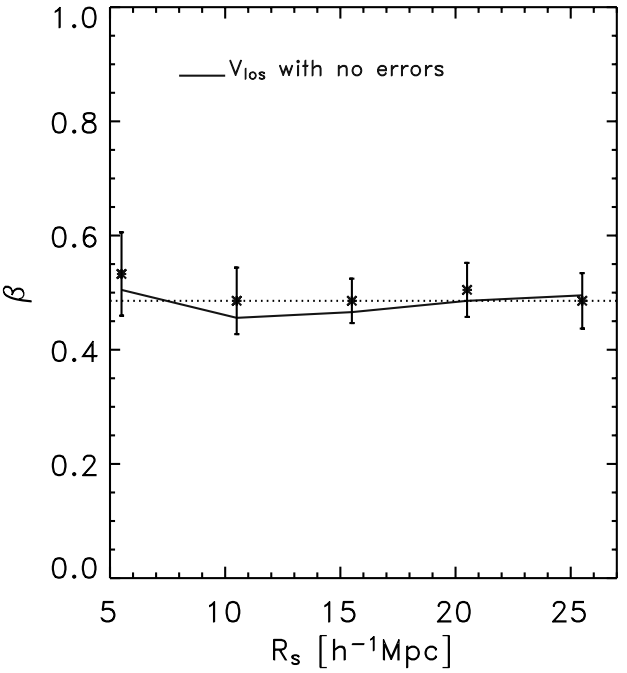

Figure 4. β as deduced from the mock 6dF catalogue as a function of smoothing radius. The stars show the mean results from 12 independent data sets and the error bars show the scatter about it. The solid line shows the result obtained from the same analysis performed using a set of noise-free mock data. The dotted line is the input value of β.

also for the quasi-linear regime. Obviously, this point needs to be explored further with many simulations and over a wide range of point separations.

4.2 Kinematic and thermal SZ clusters

Inverse Compton scattering of cosmic microwave background (CMB) photons off thermal electrons within the hot intracluster medium of galaxy clusters produces two effects: first, distortion of the CMB blackbody spectrum causing the cluster to appear brighter or dimmer at different frequencies and, secondly, an achromatic modification of its surface brightness. These effects are known, respectively, as the thermal and kinematic Sunyaev–Zel'dovich effects (Sunyaev & Zel'dovich 1972). The two combined with a measure of the cluster temperature give the radial peculiar-velocity component of the cluster to a high degree of accuracy. Current estimates of the measured distance-independent *absolute* uncertainty are as low as 130 km s^{-1} (Holder 2004).

The thermal component of the SZ effect is now routinely measured with interferometers and major efforts are underway to survey the sky within the thermal SZ relevant spectral range. Since the SZ effect is redshift independent, this kind of survey will provide an unbiased catalogue of the massive clusters as far back as their formation redshift (see, e.g. Carlstrom, Holder & Reese 2002 for a review).

The kinematic SZ is an order of magnitude weaker than the thermal component and therefore has been harder to measure (Holzapfel et al. 1997; Benson et al. 2003). In the future, however, the kinematic SZ effect will be measurable and together with the thermal SZ component will provide wide-angle surveys of galaxy-cluster peculiar velocities up to redshifts of about 2. Such data will probe the evolution of the dark energy and galaxy-cluster bias evolution and clearly distinguish between various theoretical scenarios of cosmological evolution.

Like the 6dF galaxy survey, the future SZ surveys will probe the density and the peculiar velocity of the same region of space with the same objects and therefore allow a measurement of $\Omega_{\rm m}$ (through β). The left-hand panel of Fig. 5 shows the evolution of $Hf(\Omega_{\rm m})$ as a function of redshift for different values of $\Omega_{\rm m}$ for flat ΛCDM universes normalized to the case of $\Omega_{\rm m} = 0.3$ and $\Omega_\Lambda = 0.7$. This figure demonstrates the sensitivity of the cluster SZ peculiar motions to the value of $\Omega_{\rm m}$.

The right-hand panel of Fig. 5 shows the evolution of $Hf(\Omega_{\rm m})$ as a function of redshift for various values of the dark-energy equation of state parameter, w, in a flat universe (Haiman, Mohr & Holder 2001). As pointed out by Lahav et al. (1991) the evolution of $f(\Omega_{\rm m})$ partially cancels out with the evolution in the Hubble parameter. The weak dependence of the evolution on w clearly shows that the equation of state is very hard to measure with peculiar-velocity data. On the other hand, however, this insensitivity facilitates a very accurate measurement of the cluster biasing factor and its evolution as a function of redshift.

The expected superior quality of the measured peculiar velocity of individual clusters is hampered by their sparseness. Therefore, it is essential to analyse the data with methods that are stable with respect to this feature. The method developed here is a good candidate as it is simple, easy to apply, involves no complicated inversion schemes and the vast majority of the measured clusters will satisfy the distant-observer limit assumed in the derivation. Initial application of the method to realistic mock catalogues shows good success in the recovery of the β. However, the mock data to which we applied it were at redshift zero and limited in size. When the cluster

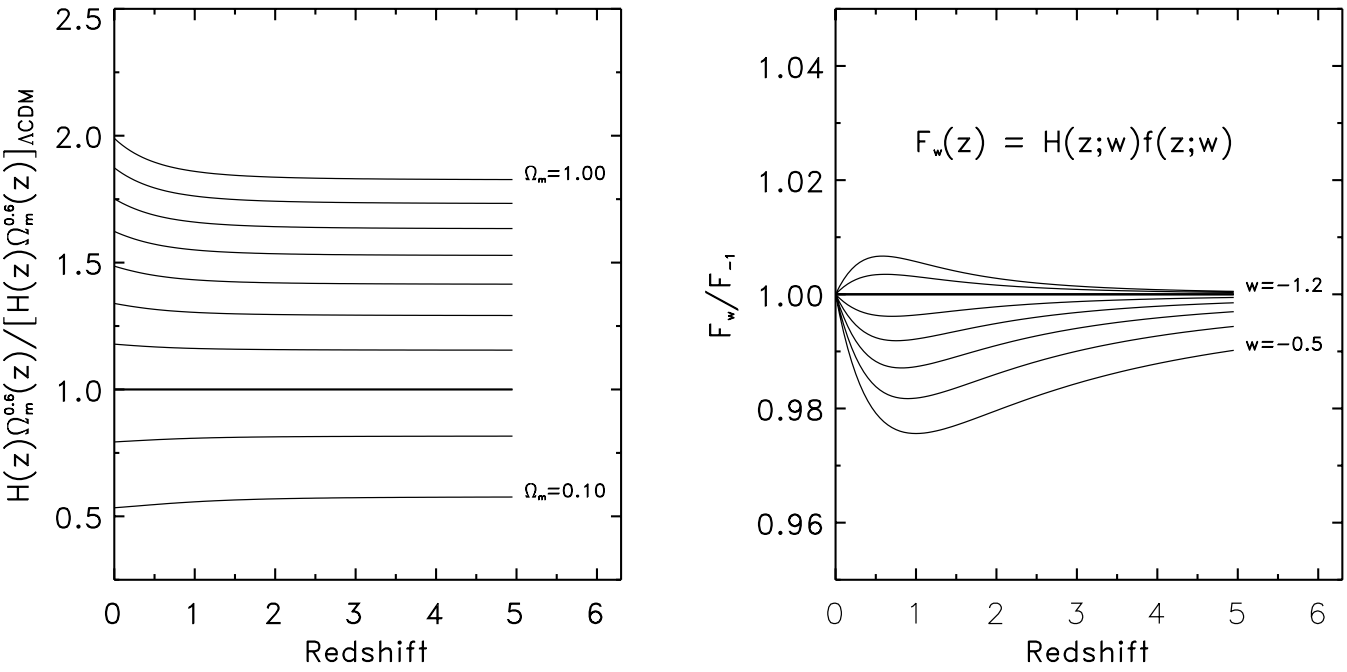

Figure 5. The left-hand panel shows the evolution of $Hf(\Omega_{\rm m})$ as a function of redshift for flat cosmological ΛCDM models with $\Omega_{\rm m} = 0.1, 0.1, \ldots, 1$, relative to the $\Omega_{\rm m} = 0.3$ and $\Omega_\Lambda = 0.7$ case. The right-hand panel shows the evolution of the same quantity as a function of redshift for different dark-energy equations of state assuming a flat ΛCDM universe with $\Omega_{\rm m} = 0.3$ and $\Omega_\Lambda = 0.7$. The lines are for the dark-energy equation of state parameter, w, values of $\{-0.6, -0.7, -0.8, -0.9, -1. -1.1, -1.2\}$, with the thick line showing the evolution in the $w = -1$ case. Although the magnitude and extremum location of the ratio vary with w, the F function itself depends very weekly on the value of w.

mass cut-off exceeds 8×10^{13} $M_\odot$ the simulation box is left with very small number of clusters. In order to test the applicability of the method properly one should apply it to very large-scale simulations that span the redshift range of 0–2, a task that will be deferred to the future.

5 DISCUSSION

In this paper we introduced the *Gaussian cell two-point 'energy-like' equation* connecting the two-point density and peculiar-velocity correlation functions. The interpretation of this equation is that the change in the velocity correlation function is caused by density variation coming from scales larger than the scale set by the Gaussian smoothing; this analytic cancellation of the small-scale power is particular to Gaussian kernels. Two practical applications of the Gaussian cell two-point energy-like equation have been developed here; the first is a direct matter power-spectrum estimator from peculiar-velocity data, and the second is β measurement from comparison of galaxy peculiar-velocity and redshift surveys. The latter application was restricted to the velocity dispersion, i.e. the $r = 0$ case.

In the $r = 0$ case, the relation derived here is similar in its mathematical form to the Irvine–Layzer cosmic energy equation. This is not surprising as each of the two relations reflect some sort of energy balance and should, due to dimensionality arguments, be homologous.

Restricting the main formula to the variance case the relation could be easily used to estimate the value of β from comparison between galaxy peculiar-velocity and redshift catalogues. In this paper we showed that despite their proximity the PSCz galaxy redshift survey and the SEcat galaxy peculiar velocity data could be reliably used to derive the value of β. The result is consistent with that of previous analyses. The variance case has also been shown to apply to the 6dF galaxy survey, despite being far from the distant-observer limit. Using mock 6dF catalogues we have demonstrated that our method can be successfully used to extract cosmological parameters from the real sample.

In the future, the eminent detectability of the kinematic Sunyaev–Zel'dovich effect will provide peculiar-velocity measurements for a large number of galaxy clusters at redshifts extending back to the formation epoch of the cluster ($z \approx 2$). This type of data is ideal to explore with the Gaussian cell two-point energy-like equation as it satisfies all of the required assumptions and has small measurement errors with large spatial coverage. The redshift coverage of the SZ data will allow an accurate measurement of the evolution of the cluster biasing factor with redshift. The main hurdle these data sets will pose is the limited resolution with which they will sample the Universe as the comoving rms distance between rich galaxy clusters is of the order of 30 h^{-1} Mpc.

We have also shown that the Gaussian cell two-point energy-like equation could be used to estimate the matter power-spectrum peculiar-velocity data in a non-parametric fashion. This is a very important application since the current measurements of the mass power spectrum from peculiar velocity employ likelihood analysis with specific models that almost certainly do not properly account for the noise contribution (Zaroubi et al. 1997, 2001). A non-parametric measurement, on the other hand, will allow a scale-by-scale dissection of the various components contributing to the measured power spectrum allowing the isolation of the noise part.

Finally, given the simplicity of equation (7) it is tantalizing to attempt to extend it to the quasi-linear regime to obtain a non-linear description of the evolution of the two-point peculiar-velocity correlation function similar to the very successful quasi-linear extension of its density counterpart (Hamilton et al. 1991). Indeed, Fig. 4

gives an encouraging indication that the equation might hold for the quasi-linear regime. This will be further explored in future work.

ACKNOWLEDGMENTS

The authors would like to acknowledge the hospitality of the Institute of Theoretical Physics, the Technion, Haifa. We would also like to thank Adi Nusser for his very insightful comments.

REFERENCES

Arfken G. B., Weber H. J., 2001, Mathematical Methods for Physicists, 5th edn. Academic Press, New York
Bardeen J. M., Bond J. R., Kaiser N., Szalay A. S., 1986, ApJ, 304, 15
Benson B. A. et al., 2003, ApJ, 592, 674
Bertschinger E., Dekel A., 1989, ApJ, 336, L5
Branchini E. et al., 2000, MNRAS, 308, 1
Carlstrom J. E., Holder G. P., Reese E. D., 2002, ARA&A, 40, 643
Cole S., Hatton S., Weinberg D., Frenk C., 1999, MNRAS, 308, 945
da Costa L. N., Bernardi M., Alonso M. V., Wegner G., Willmer C. N. A., Pellegrini P. S., Rité C., Maia M. A. G., 2000, AJ, 120, 95
Davis M., Nusser A., Willick J. A., 1996, ApJ, 473, 22
Dekel A., Bertschinger E., Faber S. M., 1990, ApJ, 364, 349
Diaferio A. et al., 2004, MNRAS, in press (doi: 10.1111/j.1365-2966.2004.08586.x) (astro-ph/0405365)
Faber S. M., Jackson R. E., 1976, ApJ, 204, 668
Feldman H. et al., 2003, ApJ, 596, L131
Ferreira P. G., Juszkiewicz R., Feldman H. A., Davis M., Jaffe A. H., 1999, ApJ, 515, L1
Fisher K., Lahav O., Hoffman Y., Lynden-Bell D., Zaroubi S., 1995, MNRAS, 272, 885
Freudling W. et al., 1999, ApJ, 523, 1
Giovanelli R., Haynes M. P., Freudling W., Da Costa L. N., Salzer J. J., Wegner G., 1998, ApJ, 505, L91
Haiman Z., Mohr J. J., Holder G. P., 2001, ApJ, 553, 545
Hamilton A. J. S., Matthews A., Kumar P., Lu E., 1991, ApJ, 374, L1
Haynes M. P., Giovanelli R., Chamaraux P., da Costa L. N., Freudling W., Salzer J. J., Wegner G., 1999, AJ, 117, 2039
Holder G. P., 2004, ApJ, 602, 18
Holzapfel W. L., Ade P. A. R., Church S. E., Mauskopf P. D., Rephaeli Y., Wilbanks T. M., Lange A. E., 1997, ApJ, 481, 35
Irvine W. M., 1961, PhD thesis, Harvard Univ.
Irvine W. M., 1965, Ann. Phys., 32, 322
Jones D. H. et al., 2004, MNRAS, 355, 747
Juszkiewicz R., Ferreira P. G., Feldman H. A., Jaffe A. H., Davis M., 2000, Sci, 287, 109
Kaiser N., 1984, ApJ, 284, L9
Kaiser N., 1987, MNRAS, 227, 1
Lahav O., Rees M. J., Lilje P. B., Primack J. R., 1991, MNRAS, 251, 128
Layzer D., 1963, ApJ, 138, 174
Layzer D., 1966, ApJ, 145, 349
Mo H. J., Jing Y. P., Börner G., 1997, MNRAS, 286, 979
Nusser A., Davis M., 1994, ApJ, 421, L1
Peebles P. J. E., 1980, The Large Scale Structure of the Universe. Princeton Univ. Press Princeton
Riess A. G., Press W. H., Kirshner R. P., 1995, ApJ, 438, L17
Saunders W. et al., 2000, MNRAS, 317, 55
Sigad Y., Eldar A., Dekel A., Strauss M. A., Yohil A., 1998, ApJ, 495, 516
Sunyaev R. A., Zel'dovich Ya. B., 1972, Comments Astrophys. Space Phys., 4, 173
Tonry J. L., 1991, ApJ, 373, L1
Tully R. B., Fisher J. R., 1977, A&A, 54, 661
Willick J. A., Strauss M. A., 1998, ApJ, 507, 64
Yahil A., Strauss M. A., Davis M., Huchra J. P., 1991, ApJ, 372, 380
Zaroubi S., 2002, MNRAS, 331, 901
Zaroubi S., Hoffman Y., Fisher K., Lahav O., 1995, ApJ, 449, 446
Zaroubi S., Zehavi I., Dekel A., Hoffman Y., Kolatt T., 1997, ApJ, 486, 21
Zaroubi S., Bernardi M., da-Costa L. N., Hoffman Y., Alonso M. V., Wegner G., Willmer C. N. A., Pellegrini P. S., 2001, MNRAS, 326, 375
Zaroubi S., Branchini E., Hoffman Y., da Costa L. N., 2002, MNRAS, 336, 1234

This paper has been typeset from a TEX/LATEX file prepared by the author.